THE ASTROPHYSICAL JOURNAL, 321:912–920, 1987 October 15

THE UNUSUAL DUST-SCATTERING PROPERTIES IN THE REFLECTION NEBULA CED 201

A. N. WITT[1]
University of Toledo
R. C. BOHLIN[1]
Space Telescope Sciences Institute
T. P. STECHER[1]
Goddard Space Flight Center
AND
S. M. GRAFF
University of Toledo
Received 1987 January 23; accepted 1987 April 6

ABSTRACT

Spectrophotometric data available from ground-based and *IUE* observations of the reflection nebula CED 201 and its illuminating star BD +69°1231 are analyzed to deduce the most likely star-nebula geometry and the wavelength dependence of the scattering characteristics of the nebular grains. The dust albedo is found to decline from 0.72 at V to probably less than 0.2 at $\lambda < 2000$ Å, explaining the unusual red color of this reflection nebula. The wavelength dependence of the optical depth and of the phase function asymmetry in the visible suggests the existence of a narrow size distribution of grains, skewed toward larger than normal particle sizes. CED 201 is one of two reflection nebulae with positive evidence for enhanced scattering in the long-wavelength wing of the 2175 Å dust extinction feature, also pointing toward larger than average grains. The cloud producing CED 201 is a small isolated molecular cloud with a density $n_H > 10^3$ cm^{-3}; the association with the star BD +69°1231 is the result of a random encounter.

Subject headings: interstellar: grains — nebulae: individual (CED 201) — nebulae: reflection — ultraviolet: spectra

I. INTRODUCTION

The study of reflection nebulae and of the stars embedded in them contributes to several important areas of astrophysical research involving interstellar grains. Foremost among these is the determination of the wavelength-dependent scattering properties of interstellar grains in the visible and the UV (e.g., Witt *et al.* 1982). Recently gaining attention has been the investigation of extended red/near-IR emission thought to originate in nonequilibrium emission processes involving small grains (Sellgren, Werner, and Dinerstein 1983) or in large polycyclic aromatic hydrocarbon molecules (Leger and Puget 1984). Finally, reflection nebulae are ideal sites for the exploration of the cloud-to-cloud variation of the interstellar extinction law as a function of wavelength (Witt, Bohlin, and Stecher 1984) made possible by the fact that many nearby reflection nebula stars experience extinction from mainly a single cloud, namely the one with which they happen to be associated.

The reflection nebula CED 201 (vdB 152) and its illuminating star BD +69°1231 are of particular interest in all three contexts. Recently Witt, Bohlin, and Stecher (1986) have shown CED 201 to be one of two cases where the UV extinction hump at 2175 Å exhibits a significant scattering component in the longward half of the band. This scattering is expected only if the band-producing particles are no longer small compared to the wavelength. At the same time, the exceptionally strong 2175 Å band seen in the spectrum of BD +69°1231 is not shifted measurably from its normal wavelength position. These two facts combine to make a strong case against graphite grains as the band-causing agents in CED 201. A quenched carbonaceous composite grain model is consistent with both findings (Onaka *et al.* 1986), because in contrast to graphite this material can produce a band at 2175 Å for a much wider range of particle sizes without a size-dependent shift of the central wavelength.

CED 201 has also been noted for exhibiting near-IR colors consistent with the presence of nonscattering emission in the R and I bands (Witt and Schild 1985). The band structure associated with this emission seen in numerous reflection nebulae in addition to CED 201 (Witt and Schild 1986*a*) has led to a tentative identification of the emission process as UV-powered luminescence by hydrogenated amorphous carbon particles (Witt and Schild 1986*b*). The CED 201 observation is important in light of the relatively late spectral type of the illuminating star (B9.5 V), because it demonstrates that hard UV radiation with $\lambda < 2000$ Å is not needed for the excitation of the near-IR emission.

Finally, Racine (1971), Glushkov and Eroshevich (1971), and Zellner (1970) all note that, contrary to conditions found in most other reflection nebulae, the color of CED 201 in the 3000–6000 Å wavelength range is *redder* than that of the illuminating star. This redness is a further indication that the particle properties in CED 201 are unusual.

The circumstances listed so far suggest that a detailed study of CED 201 may yield important information on the extent to which the scattering characteristics of grains in one interstellar cloud may deviate from the average case. In § II we examine existing surface brightness measurements of CED 201 as a

[1] Guest Observer, *International Ultraviolet Explorer* satellite, which is sponsored and operated by the National Aeronautics and Space Administration, the Science Research Council of the United Kingdom, and the European Space Agency.

basis for a radiative transfer analysis. Then, in § III, we develop a radiative transfer model suitable for explaining the surface brightness *and* color distribution at visible wavelengths, and we apply this model to the existing surface brightness data in the UV to derive limits on possible combinations of albedo and phase function for the 1300–3100 Å wavelength range. The implications of the results will be discussed in § IV and the paper will be summarized in § V.

II. OBSERVATIONAL DATA

CED 201 ($\alpha[1950.0] = 22^h12^m16^s.9$, $\delta[1950.0] = +70°00'25''$) arises in a small molecular cloud at $l = 110°.3$ and $b = +11°.4$ through the illumination by the B9.5 V star BD +69°1231. The observational data used in our study cover several aspects of this system and come from several sources.

a) *Surface Photometry in the Visible*

Racine (1971) has published an extensive set of *UBV* surface brightness data for CED 201 based on photoelectric photometry covering the offset range from 27″ to 165″ with 33 regions, each defined by a circular diaphragm of 19″ diameter. A detailed analysis of these measurements has never appeared in print. We have converted Racine's relative magnitude differences into more familiar units of relative surface brightness S/F_* (sr^{-1}) and have summarized these data in Table 1.

A second data set consisting of *BVRI* photometry of nine fields of 19″ diameter was published by Witt and Schild (1986*a*). These measurements were made with a CCD detector and are in excellent agreement with Racine's results, especially if one considers possible sources of systematic error arising from independent corrections for contributions from the night sky brightness and from instrumentally scattered starlight from the central object. Photographs of CED 201 in *B* and *I* are contained in the papers by Racine (1971) and by Witt and Schild (1986*a*), respectively.

Glushkov and Eroshevich (1971) have produced an isophotal map of CED 201 at 4740 Å as well as surface brightness profiles at the effective wavelengths 3750, 4060, and 4740 Å, based on photographic photometry. These authors qualitatively confirm the steep brightness gradient in the inner parts of CED 201, and more importantly, the notable depression of the near-UV surface brightness level compared to values at wavelengths greater than 4000 Å. This near-UV depression is also evident in Racine's data. A drop in the relative UV brightness is highly unusual for reflection nebulae, because the optical depth increases rapidly with decreasing wavelength in this spectral region.

To provide additional confirmation for this effect, one of us (A. N. W.) conducted *uvby* photometry of CED 201, using a 0.9 m telescope at the Kitt Peak National Observatory in 1981 August. A series of five concentric circular diaphragms were centered on BD +69°1231 to obtain measurements of the combined stellar and nebular flux. The stellar contribution was derived by extrapolating smoothly to zero diaphragm radius and sky corrections were obtained by observing a dark sky patch north of BD +69°1231 through the same five diaphragms. The results, expressed both as average surface brightnesses for the five circular fields centered on BD +69°1231 and, by forming differences, as average surface brightnesses of four concentric annuli centered on the star, are summarized in Table 2. Keeping in mind that these measurements represent averages over all directions from BD +69°1231, the agreement with Racine's results is excellent. Given the narrower bandpasses of the *uvby* filters, these results show the decline in the relative surface brightness for $\lambda < 4000$ Å even more clearly than do Racine's *UBV* data.

Finally, we thank Dr. R. E. Schild for providing a *V* surface brightness measurement at the same position in CED 201 which was observed with the *IUE* satellite (see § II*b*; Witt, Bohlin, and Stecher 1986). For a circular field of 10″.24 diameter positioned 20″ NE of BD +69°1231 he finds a sky- and scattering-compensated surface brightness of $\log (S/F_*) = 6.38 \pm 0.02$.

TABLE 1

RACINE'S SURFACE BRIGHTNESS DATA FOR CED 201

OFFSET (arc sec)		$\log (S/F_*)(sr)^{-1}$		
E–W	N–S	*V*	*B*	*U*
54W	...	5.16 ± 0.05	...	...
54W	27N	5.28 ± 0.04	...	...
27W	...	5.56 ± 0.02	...	...
27W	54N	5.65 ± 0.02	...	...
...	54S	4.98 ± 0.08	4.93 ± 0.10	4.97 ± 0.10
...	41S	5.45 ± 0.02	5.49 ± 0.02	5.53 ± 0.03
...	27S	5.63 ± 0.01	5.66 ± 0.02	5.68 ± 0.02
...	27N	6.21 ± 0.01	6.20 ± 0.01	6.17 ± 0.01
...	41N	5.98 ± 0.01	5.94 ± 0.01	5.90 ± 0.01
...	54N	5.74 ± 0.01	5.71 ± 0.02	5.67 ± 0.02
...	81N	5.44 ± 0.02	5.34 ± 0.02	5.28 ± 0.09
...	108N	5.00 ± 0.05	4.94 ± 0.06	4.82 ± 0.09
...	135N	4.20 ± 0.17	...	...
27E	...	6.28 ± 0.01	6.24 ± 0.01	6.20 ± 0.01
27E	54N	5.72 ± 0.01	5.66 ± 0.01	5.58 ± 0.01
27E	81N	5.40 ± 0.02	5.24 ± 0.03	5.10 ± 0.04
27E	108N	4.79 ± 0.08	4.68 ± 0.09	4.76 ± 0.10
41E	...	5.91 ± 0.01	5.90 ± 0.01	5.90 ± 0.01
54E	27S	5.54 ± 0.02	5.53 ± 0.03	5.55 ± 0.03
54E	...	5.74 ± 0.01	5.73 ± 0.01	5.71 ± 0.01
54E	27N	5.78 ± 0.01	5.72 ± 0.02	5.65 ± 0.02
54E	81N	5.06 ± 0.05	5.05 ± 0.06	4.93 ± 0.08
54E	108N	4.61 ± 0.05	4.40 ± 0.15	4.33 ± 0.20
81E	27S	5.34 ± 0.02	5.31 ± 0.03	5.28 ± 0.03
81E	...	5.40 ± 0.02	5.36 ± 0.02	5.35 ± 0.03
81E	27N	5.42 ± 0.02	5.36 ± 0.05	5.33 ± 0.06
81E	54N	5.24 ± 0.04	5.25 ± 0.05	5.13 ± 0.06
108E	27S	5.12 ± 0.04	5.04 ± 0.06	5.10 ± 0.06
108E	...	5.18 ± 0.04	5.14 ± 0.04	5.11 ± 0.04
108E	27N	5.23 ± 0.03	5.09 ± 0.04	5.00 ± 0.04
135E	...	4.89 ± 0.06	4.93 ± 0.07	4.89 ± 0.07
135E	27N	4.97 ± 0.04	4.95 ± 0.05	4.90 ± 0.06
162E	27N	4.78 ± 0.07	4.76 ± 0.08	4.56 ± 0.12

b) *Surface Photometry in the UV*

Using the *IUE* satellite (Boggess *et al.* 1978), we have obtained measurements of the surface brightness of CED 201 by placing the "large" 10″ × 20″ elliptical entrance aperture of the *IUE* spectrometer at a position 20″ NE of BD +69°1231. The short axis of the aperture was pointed toward the star. The wavelength range 1300 Å–3100 Å was covered with two exposures, SWP 26053 (420 minutes) and LWR 17726 (180 minutes) and the resulting low-resolution spectra were integrated over bands of 100 Å width. The reduction procedure is described by Witt, Bohlin, and Stecher (1986), who also provide graphical presentations of the results. We present the numerical results in Table 3, where *S* is the surface brightness of CED 201 and F_* is the flux of BD +69°1231.

TABLE 2

uvby SURFACE BRIGHTNESS DATA FOR CED 201

DIAPHRAGM RADIUS	ANNULUS LIMITS	$\langle \log (S/F_*) \rangle^a$ (sr^{-1})			
		5500 Å	4700 Å	4100 Å	3470 Å
15″.40	...	6.40 ± 0.11	6.33 ± 0.05	6.37 ± 0.03	6.15 ± 0.14
21″.11	...	6.34 ± 0.10	6.29 ± 0.06	6.29 ± 0.06	6.12 ± 0.15
28″.98	...	6.17 ± 0.08	6.16 ± 0.04	6.18 ± 0.02	6.09 ± 0.10
41″.65	...	6.01 ± 0.04	6.03 ± 0.04	6.00 ± 0.02	5.90 ± 0.08
58″.98	...	5.83 ± 0.05	5.83 ± 0.03	5.83 ± 0.03	5.72 ± 0.10
... .	15″.40 to 21″.11	6.25 ± 0.08	6.23 ± 0.08	6.19 ± 0.14	6.08 ± 0.16
... .	21″.11 to 28″.98	5.93 ± 0.04	5.96 ± 0.01	5.99 ± 0.08	6.06 ± 0.11
... .	28″.98 to 41″.65	5.75 ± 0.04	5.84 ± 0.04	5.73 ± 0.11	5.55 ± 0.18
... .	41″.65 to 58″.98	5.48 ± 0.10	5.44 ± 0.01	5.54 ± 0.14	5.43 ± 0.18

[a] The average indicates a relative surface brightness automatically averaged over all directions from BD +69°1231.

III. THE RADIATIVE TRANSFER MODEL

a) The Location of the Illuminating Star

A crucial and often most controversial part of a reflection nebula study is the determination of the position of the illuminating star relative to the scattering dust cloud. Most essential is the decision whether the star is in front of the nebula as seen by the observer or whether it is embedded in or behind the cloud. For CED 201, Racine (1971) proposed that BD +69°1231 is located in front of the scattering material. This suggestion was based solely upon the near identity in the color excess $E(B-V)$ observed for BD +69°1232, an approximately equidistant star seen about 7′ south of BD +69°1231 in a region free of any obvious nebulosity. The implied assumption is that the common reddening of $E(B-V) = 0.21$ most likely is produced by some foreground cloud and, consequently, that the dust in CED 201 does not contribute to the reddening of BD +69°1231.

More careful examination of all data now available leads to a different conclusion, however. We obtained the UV extinction curves for both stars by employing the pair method, comparing the energy distribution of BD +69°1231 and of BD +69°1232 with those of the stars ω^2 Aqr (B9.5 V, $B-V = -0.04$) and 18 Tau (B8 V, $B-V = -0.07$), respectively. The necessary observations were obtained with the *IUE* satellite. The resulting extinction curves are shown in Figure 1. The comparison indicates that the strength of the 2175 Å band in BD +69°1231 relative to the extinction in both the near- and far-UV is about 50% stronger than is found for the same band in BD +69°1232. This argues against extinction of both stars by a common foreground cloud.

TABLE 3

UV DATA FOR CED 201 AND BD +69°1231

Å	log S^a (ergs cm^{-2} s^{-1} Å^{-1} sr^{-1})	log F_* (ergs cm^{-2} s^{-1} Å^{-1})	log $(S/F_*)^a$
1300.....	−6.02 ± 0.07	−12.21	6.12 ± 0.08
1400.....	−6.14 ± 0.07	−12.02	5.88 ± 0.08
1500.....	−5.90 ± 0.04	−11.95	6.05 ± 0.05
1600.....	−6.00 ± 0.02	−11.98	5.98 ± 0.03
1700.....	−6.03 ± 0.06	−12.04	6.01 ± 0.07
1800.....	−6.01 ± 0.05	−12.08	6.07 ± 0.06
1900.....	−6.04 ± 0.03	−12.17	6.13 ± 0.04
2000.....	−6.82 ± 0.15	−12.30	5.48 ± 0.16
2100.....	−6.64 ± 0.10	−12.44	5.80 ± 0.12
2200.....	−6.69 ± 0.10	−12.53	5.84 ± 0.12
2300.....	−6.01 ± 0.09	−12.48	6.47 ± 0.10
2400.....	−5.96 ± 0.05	−12.43	6.47 ± 0.06
2500.....	−6.06 ± 0.04	−12.34	6.28 ± 0.05
2600.....	−6.13 ± 0.02	−12.30	6.17 ± 0.03
2700.....	−6.12 ± 0.02	−12.26	6.14 ± 0.03
2800.....	−6.19 ± 0.04	−12.27	6.08 ± 0.05
2900.....	−6.04 ± 0.03	−12.24	6.20 ± 0.04
3000.....	−6.03 ± 0.05	−12.22	6.19 ± 0.06
3100.....	−5.92 ± 0.07	−12.23	6.31 ± 0.08
3200.....	−5.97 ± 0.11	−12.27	6.30 ± 0.02
5500[b].....	...	...	6.38 ± 0.02

[a] For a position 20″ NE of BD +69°1231.

[b] Measurement based on CCD observation by R. E. Schild.

A further and still stronger argument in favor of a location of BD +69°1231 embedded in CED 201 comes from the surface photometry data of Racine (1971). In light of the spectral and luminosity class of BD +69°1231 and its inferred distance of about 400 pc, the surface brightness and extent of CED 201 are exceptionally high, allowing one to set some interesting limits. If the scattering is governed by the Henyey-Greenstein (1941) phase function, the observed nebular intensity in V over the range of offsets $27'' \leq r \leq 85''$ can be matched for a star in front of the nebula only for a set of extreme, probably unrealistic conditions: unit albedo; infinite optical depth per unit length, i.e., a thick nebula with diffuse reflection off the front surface; distance of the star from the front surface: 0.01 pc; and a phase function asymmetry parameter $g \leq 0.5$. A relaxation of the density condition requires abandoning a strongly forward-directed phase function, which has consistently been found to apply to the scattering in the visible.

If the star is embedded in the cloud, the angular scale corresponding to optical depth of order unity equals the apparent nebular radius, and this defines the average density in the nebula to be $n_H \approx 1.3 \times 10^3$ cm^{-3}. Assuming unit albedo and a strongly forward-directed phase function with $g = 0.85$, the observed nebular intensity requires a *minimum* optical depth $\tau_{min} = 0.46$ in V between the star and the front surface of the nebula. Assuming more realistic scattering properties forces us to conclude that essentially the entire reddening of BD +69°1231 is caused by dust in CED 201, if the star is embedded in the cloud at all. We conclude that this embedding is the only basic configuration which allows the observed surface brightness distribution in the visible to be reproduced, while assuming realistic densities and dust scattering properties.

b) Detailed Models in the Visible

Optical photographs of CED 201 (Racine 1971; Witt and Schild 1986*a*) show that BD +69°1231 is located near the SW

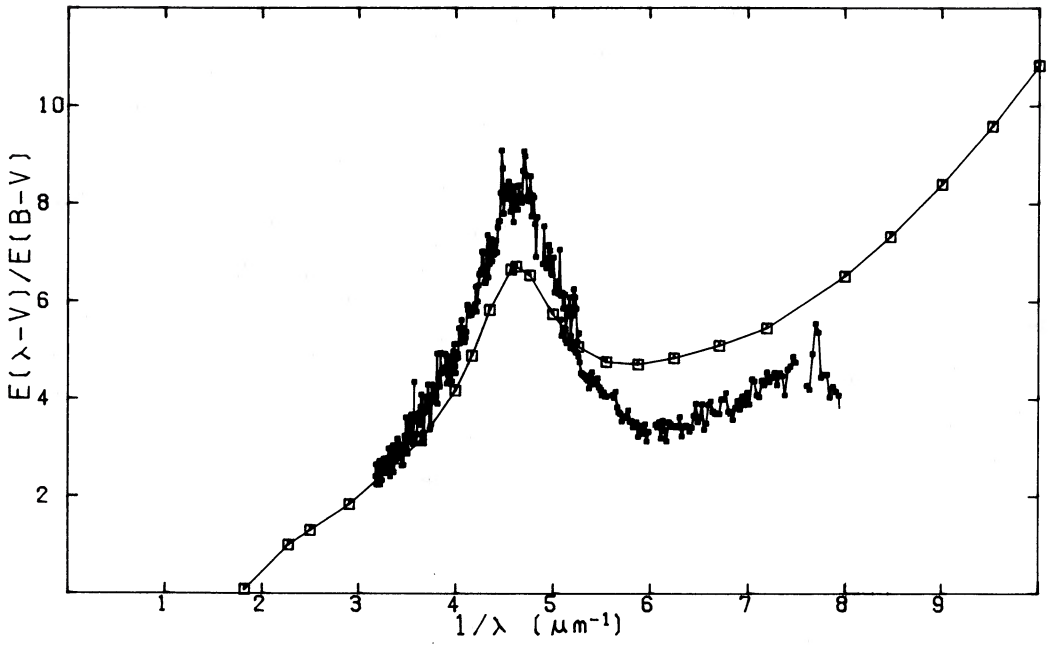

FIG. 1a

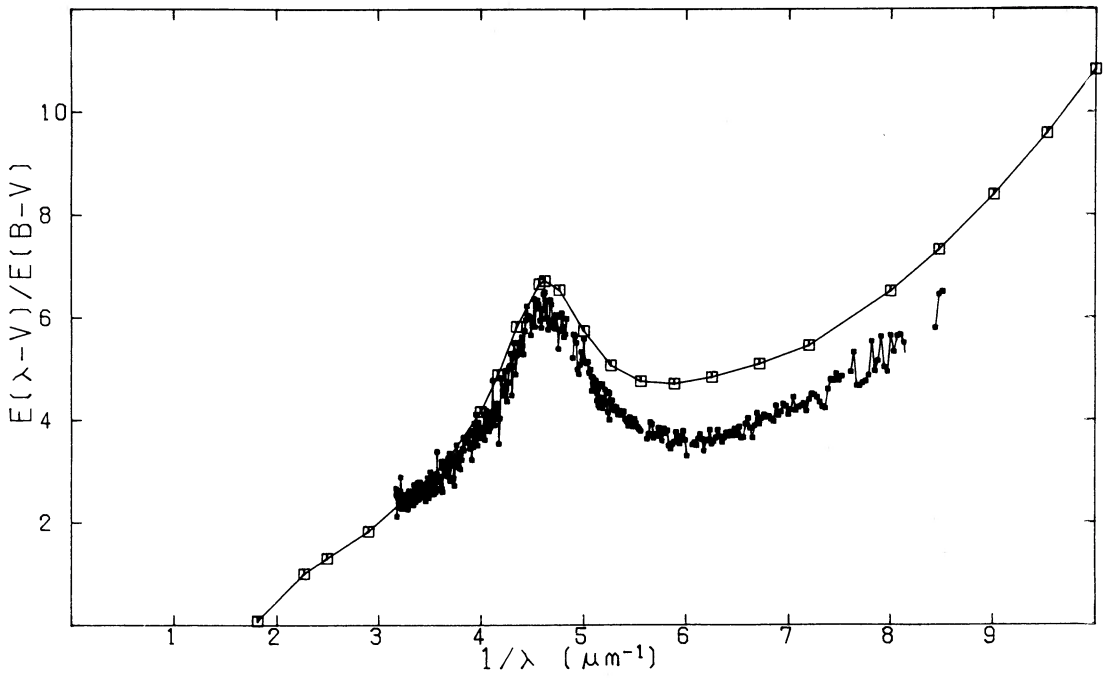

FIG. 1b

FIG. 1.—(*a*) The normalized extinction curve for BD +69°1231, the illuminating star of the reflection nebula CED 201. For comparison we display the average Galactic extinction curve of Seaton (1979) (continuous curve with squares). (*b*) The normalized extinction curve for BD +69°1232, a star located approximately 7′ south of and about equidistant with BD +69°1231.

edge of an opaque dark nebula. The level of surface brightness in CED 201 at a given offset from BD +69°1231 is highest toward the NE sector, as a consequence of this asymmetrical geometry. Since also the *IUE* data (§ II*b*) refer only to a point in this sector (at 20″ NE of BD +69°1231), we restrict the detailed modeling of the surface brightness and color data in the visible to this sector.

The purpose of calculating a detailed model for the extensive visible data set is to derive a set of geometrical parameters which can then be maintained for the analysis of the surface brightness measurements in the ultraviolet. A further constraint applied to the UV analysis is that the nebular optical depth must be scaled in accordance with the extinction curve for BD +69°1231 shown in Figure 1. We find that spherical models with centrally embedded stars and uniform density provide an excellent approximation for the surface brightness

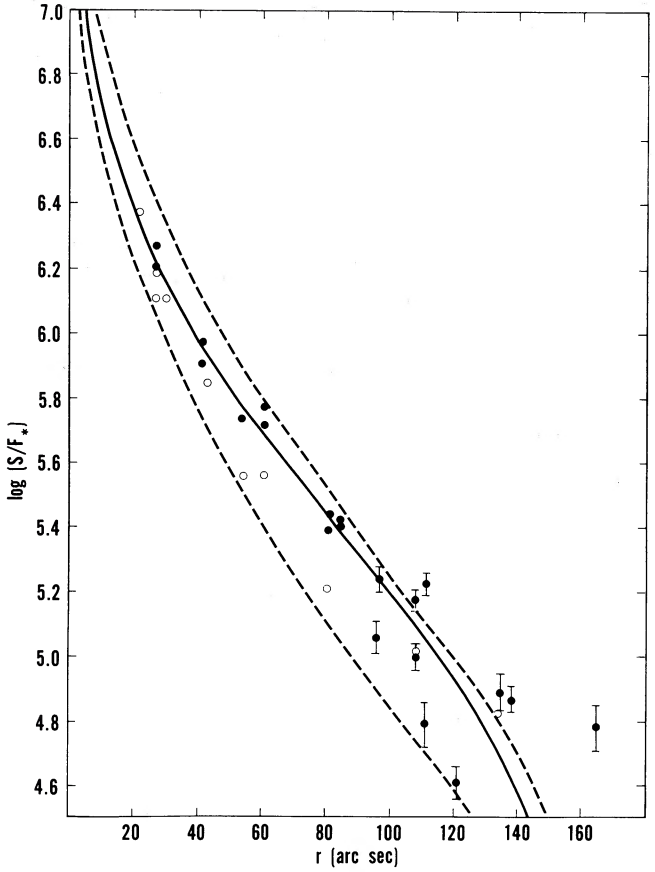

FIG. 2.—The V surface brightness distribution in the NE sector of CED 201. Filled circles are from Racine (1971) and open circles are from Witt and Schild (1986*a*). The solid curve represents the prediction from the adopted model with $\tau_V = 0.66$, $a_V = 0.72$, $g_V = 0.60$, while the upper and lower dashed curves are computations for $\tau_V = 0.88$ and for $\tau_V = 0.44$ with $a_V = 0.70$, $g = 0.70$, respectively.

distribution of any embedded star configuration, as long as the dust is forward-scattering and as long as the offsets of interest are small compared to the model radius (e.g., Witt 1977).

In Figure 2 we show V surface brightness data from Racine (1971; our Table 1) for the NE sector of CED 201 (*filled circles*), supplemented by CCD surface brightness data for the V band by Witt and Schild (1986*a*) for points in the same sector (*open circles*) as a function of offset from BD +69°1231. Shown also are three model curves derived from Monte Carlo radiative transfer calculations for a uniform spherical dust cloud of 0.3 pc radius at 400 pc distance, the distance of CED 201 inferred by Racine (1971). All significant orders of multiple scattering are included. The solid curve, deemed to represent the best fit, assumes an optical depth between the centrally embedded star and the cloud edge of $\tau = 0.66$, an albedo $a = 0.72$, and a phase function asymmetry $g = 0.60$. The two dashed curves show limiting cases with $\tau = 0.44$, $a = 0.7$, and $g = 0.7$ (*lower curve*) and with $\tau = 0.88$, $a = 0.7$, and $g = 0.7$ (*upper curve*). Given the scatter of the data points, an estimate of $\tau = 0.66 \pm 0.05$ appears a fair representation for the optical depth to the embedded star. In view of the measured color excess of $E(B-V) = 0.21$ for BD +69°1231, the derived optical depth leads to a ratio of total to selective visual extinction $R_V = 3.42 \pm 0.26$. This value is slightly larger than the galactic average for diffuse clouds of $R_V = 3.1$ and does not exclude the possibility that the reddening of BD +69°1231 includes components from nebular dust, characterized by a still larger R_V (Sherwood 1975; Whittet and van Breda 1975) and some small contribution from general diffuse cloud dust along the line of sight.

The available B observations of the NE sector of CED 201 are plotted in Figure 3. An independent fit based on the identical geometry was achieved with the parameters $\tau = 0.79$, $a = 0.60$, $g = 0.65$. A comparison with the results for V suggests that indeed the nebular dust may have a ratio $R_V = 0.66/(0.79-0.66) = 5.08$, typical for dark clouds with potentially larger dust grains. There is a significant drop in albedo in going from V to B, such that the scattering optical depth $a\tau_B$ in B is actually less than $a\tau_V$ in V, which explains the unusual red color of the nebula. The increase in g at B over the value at V is required in order to match the observed variation of the nebular-stellar color difference with offset.

This match is shown in Figure 4, where we have plotted as filled circles the color differences defined as $\Delta C(B, V) = \log (S/F_*)_B - \log (S/F_*)_V$ for all those points of Racine (1971) in the NE sector of CED 201 where the statistical accuracy is ± 0.04 in $\log (S/F_*)$ or better. Predictions based on the Monte Carlo models for B and V are shown as open circles. The statistical accuracy of the model points is comparable to that of the observations. With the same geometrical model we have also fitted Racine's U data for the NE sector of CED 201 with a similar degree of closeness. The derived parameters are $\tau_U =$

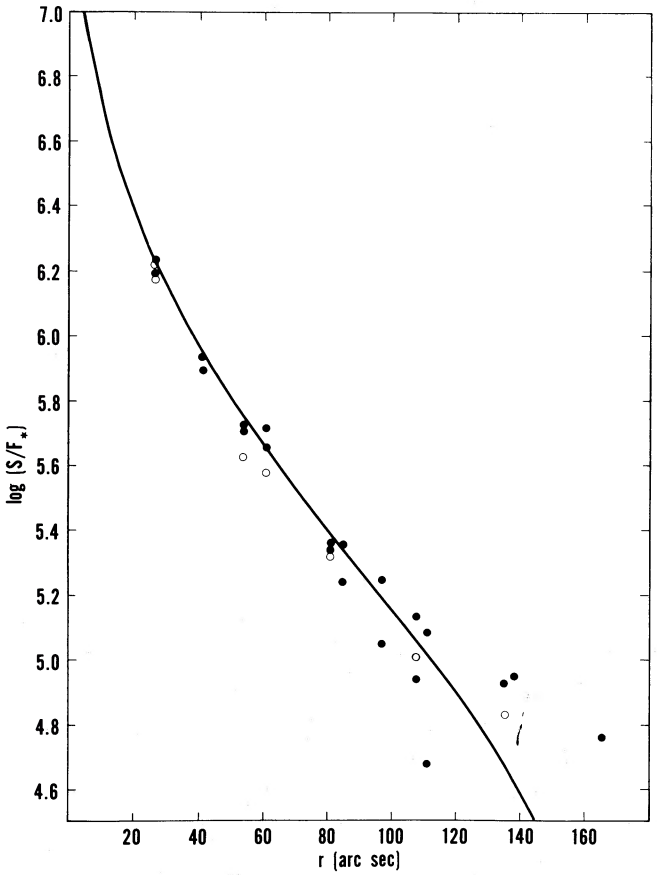

FIG. 3.—Fit of the adopted model to the observations of the B surface brightness in the NE sector of CED 201. Symbol key is the same as Fig. 2.

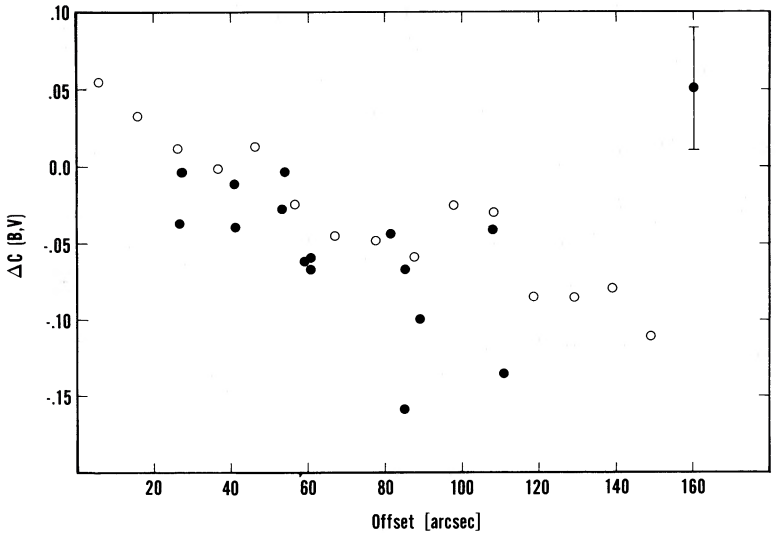

FIG. 4.—Filled circles represent color difference data for the NE sector of CED 201 derived for B, V measurements with statistical accuracy of ± 0.04 or better in log (S/F_*). Open circles are predictions derived from the adopted Monte Carlo models for B and V.

1.00, $a_U = 0.48$, and $g_U = 0.68$. The strong trend toward a lower albedo at shorter wavelengths is already well established by the UBV data.

We conclude that our model satisfactorily reproduces the visible nebular brightness distribution in CED 201 as well as the run of the nebular color with offset distance, and we will base the analysis of the UV data on the derived geometry.

c) *Analysis of the IUE Data*

Two general considerations govern the analysis of the UV surface brightness measurements of CED 201. One, the measurements compiled in Table 3 apply to a *single* nebular location only. Under these circumstances the model analysis can provide only *combinations of albedo and phase function asymmetry values* but not determinations of the two quantities separately. Two, in a nebula with optical depth near unity the scattered light at small offsets from the star is dominated by single scattering, with higher order scattering gaining increased weight only with increasing offset angles (Witt and Oshel 1977). Since we find from our detailed model that the density in CED 201 is approximately uniform, we are justified in employing a single-scattering analytical model for a uniform spherical nebula for the analysis of the IUE observations. Such a model was developed by van Houten (1961) and was further elaborated upon by Wickramasinghe (1967). This model utilizes the same Henyey-Greenstein phase function as employed in our Monte Carlo program, and in detailed comparison tests this model was found to predict about 90% of the nebular intensity produced by the multiple-scattering Monte Carlo approach.

We have used this analytical model to determine all combinations of albedo a and phase function asymmetry parameter g for the wavelengths 5500, 3000, 2800, 2600, 2500, 2400, 2300, 2200, 2100, 1900, 1800, and 1600 Å, which reproduced the corresponding measured relative surface brightness values listed in Table 3 within the stated uncertainty limits. Representative solutions are shown in Figures 5–7.

Several important conclusions can be derived from these results. The calculations for 5500 Å (Fig. 5) confirm our conclu-

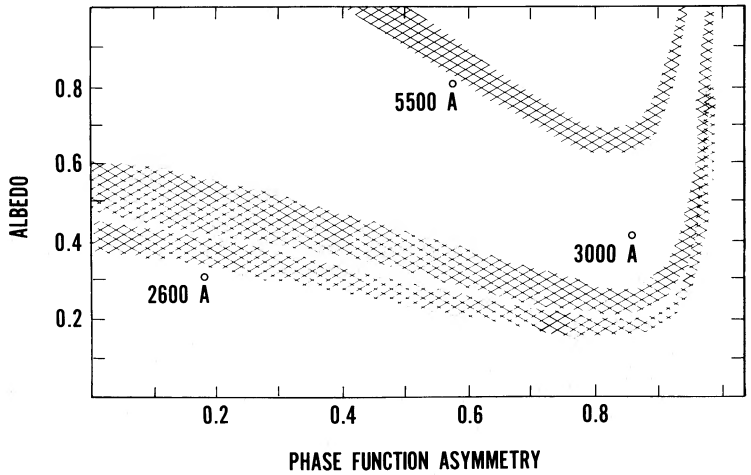

FIG. 5.—The crosshatched areas represent combinations of a and g which would reproduce the observed surface brightness at 20″NE in CED 201 in the context of our adopted model. The width of each zone reflects the uncertainties in log (S/F_*) quoted in Table 3.

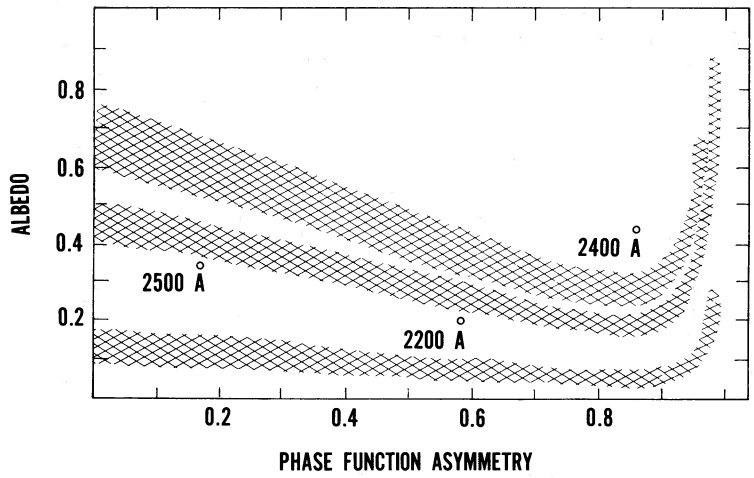

FIG. 6.—Same as Fig. 5, but for 2400–2600 Å region in CED 201

sions from the study of detailed multiple-scattering models: even when the star is embedded into the nebula at the maximum optical depth $\tau_V = 0.66$, only models with $a \geq 0.6$ and $g \geq 0.42$ can explain the very high surface brightness in the visible. Our actual solution $a_V = 0.72$ and $g_V = 0.60$ lies slightly below the crosshatched area for 5500 Å because the analytical model computes single scattering only and requires a larger albedo value than is needed for a multiple-scattering calculation to produce the same nebular intensity. All albedo values derived for the UV wavelengths are therefore upper limits to the true values.

Figure 5 also demonstrates the dramatic decline in the likely particle albedo with decreasing wavelength between 5500 Å and 2600 Å. An indication of this trend was already apparent in the detailed models for *V*, *B*, and *U* with $a = 0.72$, 0.60, and 0.48, respectively. The value of the phase function asymmetry factor g in the UV is unconstrained by the *IUE* observations, but if the trend apparent in *V* and *B* may be extrapolated, g-values in the range 0.6–0.8 are possible, which leads to the conclusion that the albedo at 2600 Å has the unusually low value of approximately 0.2.

Figure 6 illustrates the enhanced scattering associated with the long-wavelength wing of the 2175 Å interstellar band, an effect first detected in the reflection nebulae CED 201 and IC 435 by some of us (Witt, Bohlin, and Stecher 1986). The albedo at 2400 Å and at 2300 Å is roughly 50% higher than the albedo at 2500 Å and is approximately triple the value at 2200 Å. The significant relative increase in particle albedo between the wavelengths 2600 and 2300 Å becomes detectable only because the base albedo at 2600 Å is so low in CED 201. The extremely low albedo at 2200 Å confirms the essential absorption nature of the 2175 Å band.

Figure 7 shows that the albedo shortward of the 2175 Å undergoes a moderate rise. The band of solutions for 1800 Å is representative of the entire 1300 Å to 1800 Å region.

d) The Uncertain UV Phase Function

As stated earlier, surface brightness measurements at only one offset angle generally do not place very effective limits on dust scattering properties. Figures 5 to 7 demonstrate that this is particularly true for the phase function asymmetry in the UV. The crosshatched area in Figure 8 represents the *IUE* observations for the 1600 Å–1800 Å spectral region in CED 201. The two curves are computed from our adopted standard model, using the Monte Carlo multiple-scattering approach, for parameters $\tau = 1.34$, $a = 0.30$, $g = 0.20$ (*solid curve*), and $\tau = 1.34$, $a = 0.16$, $g = 0.85$ (*dashed curve*). Both are acceptable solutions, but they differ greatly in the predicted surface bright-

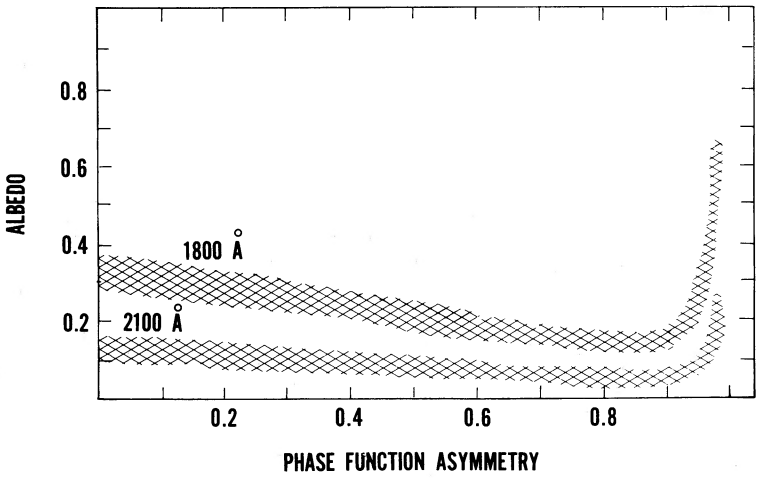

FIG. 7.—Same as Fig. 5, but for 2100–1800 Å region in CED 201

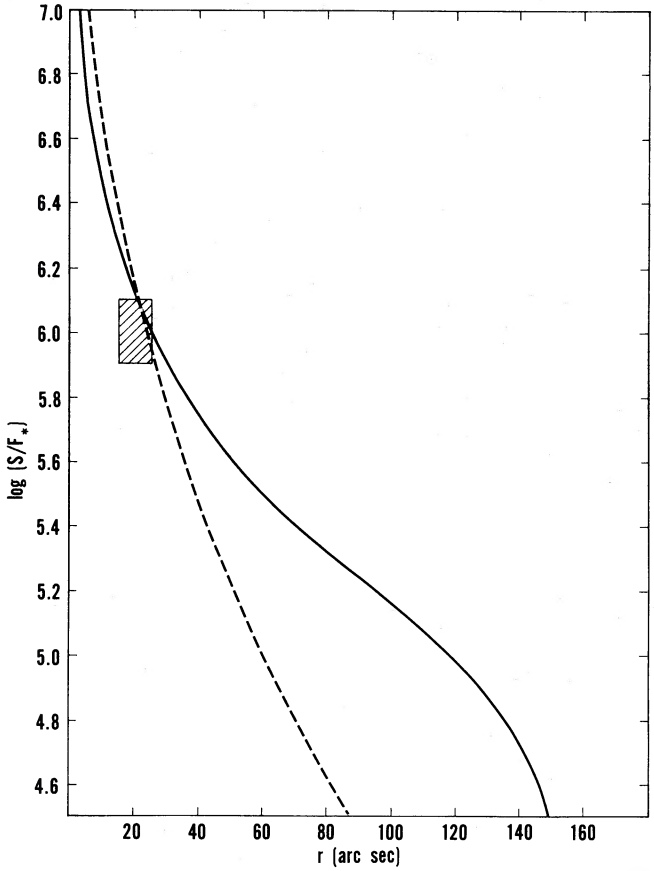

FIG. 8.—Examples of two possible solutions for the observed surface brightness at 20″NE in CED 201 in the 1600–1800 Å region. The solid curve represents near-isotropic scattering with $\tau = 1.34$, $a = 0.30$, $g = 0.20$, while the dashed curve reflects a strongly forward-directed case with $\tau = 1.34$, $a = 0.16$, $g = 0.85$.

ness at offset angles greater than 20″. One requires sensitive means to measure UV surface brightnesses one order of magnitude fainter than the *IUE* measurement to distinguish observationally between the illustrated cases.

IV. DISCUSSION

The dust properties in CED 201 as derived from the available observations appear unusual in several ways. First, the red color of CED 201 in the visible, noted by several observers, is peculiar. The great majority of reflection nebulae are bluer than their illuminating stars in this spectral region (see, e.g., Witt and Schild 1986*a*). Detailed studies of individual nebulae have revealed an essentially constant albedo in the 3000 Å to 5500 Å range, e.g., in NGC 2023 (Witt, Schild, and Kraiman 1984), in NGC 7023 (Witt and Cottrell 1980), or in the Merope nebula (Witt 1985), and similar results have emerged from the study of the diffuse galactic light (Lillie and Witt 1976) and of scattering by isolated dense interstellar clouds (FitzGerald, Stephens, and Witt 1976). In this setting the decline of the albedo in CED 201 by 33% between the V and the U band is highly unusual. The change to an increasingly forward-scattering phase function with decreasing wavelength ($g_V = 0.60$, $g_B = 0.65$, $g_U = 0.68$) strongly suggests that the particles responsible for the visible scattering in CED 201 must have a narrow size distribution, strongly skewed toward larger, wavelength-sized grains. We note that the rather broad power-law size distribution of graphite and silicate grains proposed by Draine and Lee (1984) predicts an essentially constant phase function asymmetry in this spectral region. The normally more numerous smaller grains, scattering in the ultraviolet and providing a moderate albedo and a somewhat less forward-directed phase function there, do not appear to be present in CED 201. Instead, as confirmed by our *IUE* observations, the UV is dominated largely by absorbing grains.

The 2175 Å extinction band is of unusual strength in CED 201, as is shown in Figure 1*a*. It is not clear whether the scattering observed in the long-wavelength wing of the 2175 Å band (Witt, Bohlin, and Stecher 1986) in CED 201 is an exceptional characteristic of the grains encountered here or whether its detection is favored by the otherwise low albedo in the UV coupled with the strength of the band. Examination of the *IUE* spectra of other reflection nebulae (Cardelli and Bohm 1984) makes it appear likely that NGC 1999, NGC 1432, and the Electra nebula are other cases where scattering in the long-wavelength side of the 2175 Å band may be evident, in addition to IC 435 already found by some of us. Such scattering is a characteristic of particles larger than the classical Rayleigh limit, probably larger than the narrow size range permitted for graphite grains in order to produce the 2175 Å band via a surface plasmon resonance. We note the recent work by Onaka *et al.* (1986) who show that grains of quenched carbonaceous composite material can range over a considerable interval of sizes without leading to a noticeable shift in the center of the 2175 Å feature produced by them.

Given that most bright reflection nebulae are the result of close associations of dense interstellar clouds with young stars apparently formed in them (Witt and Schild 1986*a*), we need to examine how a not obviously young BD +69°1231 has come to illuminate the nebula CED 201. Kutner *et al.* (1980) have detected CED 201 in the microwave radiation of ^{12}CO and ^{13}CO at the position of BD +69°1231. They found LSR radial velocities of -5.3 km s^{-1} and -5.2 km s^{-1}, respectively. Their radio map confirms the scattering result in placing the density peak of the CED 201 cloud to the NE of BD +69°1231. We are grateful to Dr. Helmut A. Abt for having measured the radial velocity of BD +69°1231 for us. He finds (private communication, 1978) on the basis of six spectra an essentially constant heliocentric radial velocity of -28.9 ± 3.0 km s^{-1}. This converts to a LSR velocity of -17.0 ± 3.0 km s^{-1} for BD +69°1231. Hence, with a relative velocity of 11.7 km s^{-1} and a typical radius for CED 201 of 0.3 pc, BD +69°1231 could have moved to its present location from outside the nebula in less than 3×10^4 yr. CED 201 is probably the result of an accidental encounter of BD +69°1231 with a small, dense molecular cloud.

V. SUMMARY

1. We collected available surface brightness measurements of the reflection nebula CED 201. The data in the visible provide excellent spatial coverage, and they reveal that CED 201 is generally redder than the illuminating star, BD +69°1231.

2. The surface brightness and color data in the visible provide tight constraints on the possible geometry of the star-nebula arrangement. A model with the star embedded into the nebula by the maximum amount permitted by the star's color excess leads to the most realistic solution.

3. A multiple-scattering Monte Carlo model suggests that

the dust albedo declines by about 33% from V to U in the visible, while the phase function asymmetry increases notably with decreasing wavelength in the visible. This suggests a fairly narrow size distribution with a preponderance of larger grains contributing to the scattering in the visible.

4. The relative UV surface brightness of CED 201, as determined from *IUE* spectra at 20″ NE of BD +69°1231, is well below the corresponding visual value of S/F_*. While the lack of adequate spatial coverage in the UV prevents an independent determination of both albedo and phase function asymmetry, the dust albedo in this nebula is likely to be unusually low ($a \sim 0.2$) throughout most of the UV when compared with $a \approx 0.5$–0.6 typical for other reflection nebulae and the general diffuse galactic light.

5. Enhanced scattering is detected in the long-wavelength wing of the 2175 Å dust extinction feature, which is exceptionally strong in CED 201. The central wavelength of the feature is not notably shifted toward longer wavelengths, as expected for larger sized graphite grains. This finding may be evidence that the feature is caused by amorphous carbon grains.

6. Radial velocity measurements of both the nebula CED 201 and the star BD +69°1231 make it almost certain that this reflection nebula is the result of an accidental encounter of a small dense molecular cloud with an unrelated star.

Thanks are due to the *IUE Observatory* staff at the Goddard Space Flight Center for their contributions in obtaining the UV data used in this investigation. We are grateful to R. E. Schild for obtaining a V surface brightness measurement at the *IUE* position in CED 201, and to H. A. Abt for providing crucial radial velocity measurements for BD +69°1231. We also acknowledge the assistance of J. B. Kraiman in the early stages of the analysis. Material support was obtained from the National Aeronautics and Space Administration through grants NAG5-467 and NAGW-89 to The University of Toledo.

REFERENCES

Boggess, A., *et al.* 1978, *Nature*, **275**, 327.
Cardelli, J. A., and Bohm, K. H. 1984, *Ap. J.*, **285**, 613.
Draine, B. T., and Lee, H. M. 1984, *Ap. J.* **285**, 89.
FitzGerald, M. P., Stephens, T. C., and Witt, A. N. 1976, *Ap. J.*, **208**, 709.
Glushkov, Y. I., and Eroshevich, E. S. 1971, *Trudy Astrofiz. Inst. Alma Ata*, **16**, 13.
Henyey, L. G., and Greenstein, J. L. 1941, *Ap. J.*, **93**, 76.
Kutner, M. L., Machnik, D. E., Tucker, K. D., and Dickman, R. L. 1980, *Ap. J.*, **237**, 734.
Léger, A., and Puget, J. L. 1984, *Astr. Ap.*, **137**, L5.
Lillie, C. F., and Witt, A. N. 1976, *Ap. J.*, **208**, 64.
Onaka, T., Nakada, Y., Tanabe, T., Sakata, A., and Wada, S. 1986, *Ap. Space Sci.*, **118**, 411.
Racine, R. 1971, *A.J.*, **76**, 321.
Seaton, M. J. 1979, *M.N.R.A.S.*, **187**, 739.
Sellgren, K., Werner, M. W., and Dinerstein, H. L. 1983, *Ap. J.* (*Letters*), **271**, L13.
Sherwood, W. A. 1975, *Ap. Space Sci.*, **34**, 3.
van Houten, C. J. 1961, *Bull. Astr. Inst. Netherlands*, **16**, 1.
Whittet, D. C. B., and van Breda, I. G. 1975, *Ap. Space Sci.*, **38**, L3.
Wickramasinghe, N. C. 1967, *Interstellar Grains* (London: Chapman & Hall).
Witt, A. N. 1985, *Ap. J.*, **294**, 216.
———. 1977, *Ap. J. Suppl.*, **35**, 21.
Witt, A. N., Bohlin, R. C., and Stecher, T. P. 1984, *Ap. J.*, **279**, 698.
———. 1986, *Ap. J.* (*Letters*), **305**, L23.
Witt, A. N., and Cottrell, M. J. 1980, *A.J.*, **85**, 22.
Witt, A. N., and Oshel, E. R. 1977, *Ap. J. Suppl.*, 35, 31.
Witt, A. N., and Schild, R. E. 1985, *Ap. J.*, **294**, 225.
———. 1986*a*, *Ap. J. Suppl.*, **62**, 839.
———. 1986*b*, in *Proc. Summer School on Interstellar Processes*, ed. D. Hollenbach and H. A. Thronson, Jr., in press.
Witt, A. N., Schild, R. E., and Kraiman, J. B. 1984, *Ap. J.*, **281**, 708.
Witt, A. N., Walker, G. A. H., Bohlin, R. C., and Stecher, T. P. 1982, *Ap. J.*, **261**, 492.
Zellner, B. H. 1970, Ph.D. thesis, University of Arizona.

RALPH C. BOHLIN: Space Telescope Science Institute, Homewood Campus, Baltimore, MD 21218

STEPHEN M. GRAFF: Department of Physics, University of Notre Dame, Notre Dame, IN 46556

THEODORE P. STECHER: NASA-Goddard Space Flight Ctr., Code 680, Greenbelt, MD 20771

ADOLF N. WITT: Ritter Observatory, The University of Toledo, Toledo, OH 43606